Modification of magnetic anisotropy through $3d$-$4f$ coupling in $La_{0.75}Pr_{0.25}Co_2P_2$

Kirill Kovnir,[1,*] Corey M. Thompson,[1,†] V. Ovidiu Garlea,[2] Daniel Haskel,[3] Anatolii A. Polyanskii,[4] Haidong Zhou,[4,‡] and Michael Shatruk[1,4,§]

[1]*Department of Chemistry and Biochemistry, Florida State University, Tallahassee, Florida 32306, USA*
[2]*Quantum Condensed Matter Division, Oak Ridge National Laboratory, Oak Ridge, Tennessee 37831, USA*
[3]*Advanced Photon Source, Argonne National Laboratory, Argonne, Illinois 60439, USA*
[4]*National High Magnetic Field Laboratory, Florida State University, Tallahassee, Florida 32306, USA*

(Received 3 June 2013; revised manuscript received 25 July 2013; published 30 September 2013)

Magnetic behavior of $La_{0.75}Pr_{0.25}Co_2P_2$ was investigated by a combination of magnetic measurements, magneto-optical imaging, neutron diffraction, and x-ray absorption spectroscopy, including x-ray magnetic circular dichroism. The material crystallizes in the $ThCr_2Si_2$ structure type and exhibits three consecutive magnetic phase transitions. At 167 K, the Co magnetic moments order ferromagnetically in the *ab* plane of the tetragonal crystal structure. At 66 K, a ferromagnetic ordering of Pr($4f$) moments parallel to the *c* axis causes a rotation of the Co($3d$) moments towards the *c* axis in the direction opposite to the Pr moments, thus forming a noncollinear ferrimagnetically ordered structure and switching the direction of the total magnetization from the *ab* plane to the *c* axis. The third magnetic transition observed at 35 K is likely associated with the establishment of the collinear ferrimagnetic order along the *c* axis.

DOI: 10.1103/PhysRevB.88.104429 PACS number(s): 75.50.Gg, 75.30.Gw, 78.20.Ls

I. INTRODUCTION

Interest in materials of the $ThCr_2Si_2$ structure type, one of the most ubiquitous atomic arrangements for ternary intermetallic compounds, has been reinvigorated recently due to the discovery of high-temperature superconductivity in doped $BaFe_2As_2$.[1,2] The unconventional behavior observed for this class of superconductors[3] calls for active exploration of the interplay between the electronic and crystal structures and the transport and magnetic properties in related itinerant systems. Although ternary intermetallics often demonstrate intrinsically complex crystal structures,[4] those that belong to the $ThCr_2Si_2$ structure type can be conveniently represented as materials built of alternating A and $[T_2X_2]$ layers (Fig. 1), where A = alkali, alkali-earth, rare-earth, or actinide metal; T = transition metal; and X = nonmetal. In addition, materials with layered arrangements of magnetic moments are also of great interest due to their tendency to exhibit highly anisotropic magnetic behavior.

Compounds of the $ThCr_2Si_2$ type were studied extensively ~2–3 decades ago, when Zheng and Hoffmann proposed a simple and effective theoretical approach to explain structural changes observed in such solids as a function of electron count.[5] A more rigorous theoretical analysis was developed later by Johrendt *et al.*[6] Many experimental studies focused on elaborating the rich magnetic behavior of RMn_2Si_2 and RMn_2Ge_2 compounds (R = rare earth),[7] especially after the report of reentrant ferromagnetism in $SmMn_2Ge_2$ by Fujii *et al.*[8]

Reehuis *et al.* carried out a comprehensive study of the structural and magnetic properties of ternary RCo_2P_2 materials,[9–12] which are closely related to the aforementioned superconducting pnictides. Recently, we and other groups have demonstrated that the magnetic properties of the $ThCr_2Si_2$-type phosphides[13–17] can be as rich and diverse as those of the aforementioned silicides and germanides, provided that proper iso- and aliovalent substitutions are made to modify the crystal and electronic structures of the materials. In particular, we focused on the drastically different magnetic properties of $LaCo_2P_2$ and $PrCo_2P_2$, which exhibit ferromagnetic (T_C = 132 K) and antiferromagnetic (T_N = 305 K) ordering in the Co sublattice, respectively.[13] In both cases, a ferromagnetic arrangement of magnetic moments within the square plane of Co atoms is observed. In $LaCo_2P_2$, the Co moments are aligned in plane and parallel to the moments in the other layers, leading to the ferromagnetic ground state.[10] In $PrCo_2P_2$, they are aligned perpendicular to the plane (along the *c* axis), but antiparallel magnetic coupling between neighboring planes results in antiferromagnetism.[11] The change in the type of magnetic ordering was attributed to the strong shortening of the interplanar P–P distances upon going from $LaCo_2P_2$ (3.16 Å) to $PrCo_2P_2$ (2.57 Å). We have demonstrated, however, that ferromagnetic ordering of Co moments in mixed $La_{1-x}Pr_xCo_2P_2$ phases can be sustained even at rather high levels of Pr content and relatively short P–P distances (x = 0.75 and 2.67 Å, respectively).[13] Moreover, we showed that the increase in the Curie temperature for higher Pr content (up to T_C = 268 K for x = 0.75) stems from the increase in the intraplanar Co–Co distances that causes stronger spin polarization of the electronic band structure at the Fermi level.

$PrCo_2P_2$ also exhibits an antiferromagnetic transition at 19 K due to the ordering in the Pr sublattice. Interestingly, a similar antiferromagnetic-like transition in the mixed $La_{1-x}Pr_xCo_2P_2$ phases, with lower Pr content, occurs at a substantially higher temperature (>50 K).[13] One may hypothesize that the persistence of the ferromagnetic state of the Co sublattice in these materials can create a sufficient internal field to cause ordering of the Pr moments at a higher temperature than is possible in pure $PrCo_2P_2$, where the Co sublattice is antiferromagnetic below 305 K. Furthermore, one may question whether the change in the magnetic anisotropy of the Co sublattice from the easy-axis type in $PrCo_2P_2$ to the easy-plane type in $LaCo_2P_2$ is related to the existence of anisotropic magnetic moments in the rare-earth sublattice of the former. To shed more light on

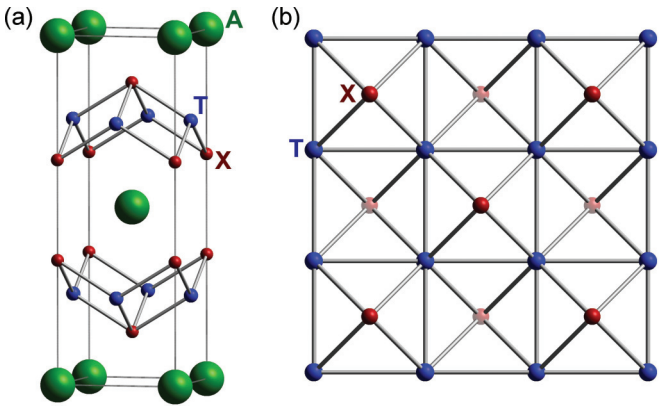

FIG. 1. (Color online) (a) Crystal structure of AT_2X_2 that belongs to the $ThCr_2Si_2$ structure type. (b) Top view of the square planar net of T atoms, with X atoms positioned above and below the net in a chessboardlike fashion.

the magnetic anisotropy in the mixed quaternary phases and on the nature of the low-temperature magnetic transition, we embarked on the study of a representative compound, $La_{0.75}Pr_{0.25}Co_2P_2$. Reported herein is a detailed investigation of its structural and magnetic properties that demonstrates the strong temperature-dependent magnetic anisotropy of this material and its low-temperature ferrimagnetism. By combining magnetic measurements, magneto-optical imaging (MOI), neutron diffraction, and x-ray absorption spectroscopy, we demonstrate the antiparallel alignment of Co and Pr magnetic moments in the magnetically ordered ground state of $La_{0.75}Pr_{0.25}Co_2P_2$.

II. EXPERIMENTAL METHODS

Finely dispersed powders of lanthanum (99.9%), praseodymium (99.9%), and red phosphorus (99.999%), as well as tin shots (99.99%), were obtained from Alfa Aesar and used as received. Cobalt powder (Alfa Aesar, 99.5%) was additionally purified by heating under a flow of H_2 gas at 775 K for 5 h. All manipulations during sample preparation were carried out in an argon-filled dry box (content of $O_2 < 1$ ppm).

$La_{0.75}Pr_{0.25}Co_2P_2$ was prepared by annealing a mixture of elements in tin flux, as reported earlier,[13] but the reaction was scaled up to obtain a sufficient amount of material for neutron diffraction studies. The total weight of the sample was 25 g, of which 22.5 g was Sn flux. The reaction was performed in an evacuated and sealed silica tube with a 20-mm inner diameter. The temperature was raised to 1150 K in a span of 24 h and maintained constant for 10 days. Then the reaction tubes were removed from the furnace and allowed to cool to room temperature. The tin matrix was removed by soaking the sample in dilute hydrochloric acid (1:1 v/v). At this point, large single crystals ($5 \times 5 \times 0.1$ mm^3) were selected from the sample for physical property measurements. The La/Pr ratio of 0.75:0.25 was confirmed by energy-dispersive x-ray microanalysis on a JEOL 5900 scanning electron microscope.

The phase purity of the bulk product obtained by the described synthetic procedure was confirmed by powder x-ray diffraction on a Rigaku DMAX 300 Ultima III diffractometer (CuKα, $\lambda = 1.54185$ Å), with Ge as an internal standard. Variable-temperature powder x-ray diffraction data were collected on an original setup based on a Huber imaging plate Guinier camera 670 (CuKα_1, $\lambda = 1.54060$ Å) with a Ge crystal monochromator. Data were collected at a 0.005° resolution in the temperature range of 10–300 K by employing a closed-cycle He refrigeration system. The unit cell parameters were calculated by least-squares fitting with the WinCSD software package.[18]

The heat capacity and electrical resistivity were measured with a Quantum Design Physical Property Measurement System in the temperature range of 1.8–300 K. The heat capacity was measured on a pellet produced by annealing a cold-pressed polycrystalline sample at 1073 K for 72 h. To obtain the magnetic component of the heat capacity, the nonmagnetic contribution was subtracted by measuring paramagnetic $LaFe_{0.5}Co_{1.5}P_2$ as a nonmagnetic standard.[15] Electrical resistivity measurements were carried out on a single crystal of $La_{0.75}Pr_{0.25}Co_2P_2$ using the standard four-point alternating current (ac) method under magnetic fields of 0, 3, and 9 T.

Magnetic measurements were performed on an oriented single crystal of $La_{0.75}Pr_{0.25}Co_2P_2$ with a Quantum Design superconducting quantum interference device (SQUID) magnetometer MPMS-XL. Direct current magnetic susceptibility measurements were carried out in an applied field of 0.01 T in the 1.8–350 K range. Magnetization and hysteresis were measured with the magnetic field varying from -7 to 7 T.

Magneto-optical imaging was performed by placing a Bi-doped garnet indicator film with in-plane magnetization on an as-grown surface of a single crystal of $La_{0.75}Pr_{0.25}Co_2P_2$. The strong magneto-optical Faraday effect in garnet films allowed visualization of the domain structure of the material in a polarized optical microscope. The sample was installed on the cold finger of a continuous-flow optical cryostat, and tight temperature contact between the sample and the cold finger was provided by a silicone heat sink. A silicon diode, in conjunction with a LakeShore temperature controller, was used to provide stable measurement temperatures. The cryostat containing the sample and magnetic indicator film was mounted on the stage of a conventional optical microscope operating in the reflection mode and equipped with a charge-coupled device digital camera for image acquisition. Two external solenoids were used to apply vertical and in-plane magnetic fields (parallel and perpendicular to the c axis, respectively) up to ~180 mT. Variable-temperature images were recorded in this experimental setting.

Neutron scattering experiments on $La_{0.75}Pr_{0.25}Co_2P_2$ were carried out on the HB-2A high-resolution neutron powder diffractometer at the High Flux Isotope Reactor at Oak Ridge National Laboratory. The sample was held in a cylindrical vanadium container in a top-loading closed-cycle refrigerator. Two different wavelengths, $\lambda = 1.536$ and 2.410 Å, were produced by (115) and (113) reflections, respectively, from a vertically focusing Ge monochromator. The data were acquired in the temperature range of 4–220 K by scanning the detector array consisting of 44 ^{3}He tubes in two segments to cover the total 2θ range of 4°–150° in steps of 0.05°. Overlapping detectors for the given step were used to average the counting efficiency of each detector. More details about the HB-2A instrument and data collection strategies can be found in the original publication.[19]

To elucidate order parameters for magnetic phase transitions and for more accurate modeling of the magnetic structure, selected magnetic and nuclear reflections were additionally scanned on the HB-1A fixed-incident-energy ($\lambda = 2.36$ Å) triple-axis spectrometer equipped with a double pyrolytic graphite (PG) monochromator system. Highly oriented PG filters were used to minimize higher-order contaminations of the beam.

X-ray absorption near-edge structure (XANES) and x-ray magnetic circular dichroism (XMCD) spectra were collected at beamline 4-ID-C of the Advanced Photon Source, Argonne National Laboratory. The measurements were performed in helicity switching mode (1 Hz) using a 7-T superconducting cryomagnet with a variable-temperature insert. X-ray energy was tuned to near the Co L_2 and L_3 edges (793 and 778 eV, respectively) and the Pr M_4 and M_5 edges (948 and 928 eV, respectively) to probe the magnetic polarization of the Co $3d$ and Pr $4f$ states as dictated by dipole selection rules. Further details of the XMCD setup are available elsewhere.[20]

III. CRYSTAL STRUCTURE

As shown by our earlier single-crystal x-ray investigation,[13] $La_{0.75}Pr_{0.25}Co_2P_2$ crystallizes in the $ThCr_2Si_2$ structure type (space group $I4/mmm$), in which layers of rare-earth atoms alternate with slabs of $[Co_2P_2]$ composition. The latter can be viewed as a square planar net of Co atoms, with P atoms capping the centers of squares on both sides of the plane in a chessboardlike fashion (Fig. 1). No superstructure reflections were observed in diffraction patterns, suggesting that the La and Pr atoms are statistically distributed over the rare-earth sites. This structural model was confirmed by high-resolution neutron diffraction experiments performed at 220 K. The Rietveld refinement of the neutron diffraction pattern converged to the composition $La_{0.79(4)}Pr_{0.21(4)}Co_2P_2$, in good agreement with the nominal one. Unit cell parameters obtained by single-crystal and powder x-ray diffraction and neutron powder diffraction (NPD) are provided for comparison in Table I.

Variable-temperature x-ray powder diffraction experiments reveal that the unit cell volume gradually decreases as the temperature is lowered.[13] Unit cell parameters a and c, however, exhibit anomalous behavior (Fig. 2). Parameter a decreases and parameter c increases upon lowering the temperature, but a turning point is observed at ~170 K, below which the a and c parameters begin to increase and decrease, respectively. As will be shown below, these changes are associated with a magnetic phase transition.

TABLE I. Unit cell parameters and volume of $La_{0.75}Pr_{0.25}Co_2P_2$ determined by various methods.

Diffraction method	a (Å)	c (Å)	V (Å^3)
X-ray single crystal[a]	3.8260(1)	10.9031(3)	159.603(7)
X-ray powder[a]	3.8225(2)	10.891(2)	159.13(2)
Neutron powder[b]	3.81574(4)	10.8749(1)	158.337(3)

[a]Measured at room temperature.
[b]Measured at 220 K.

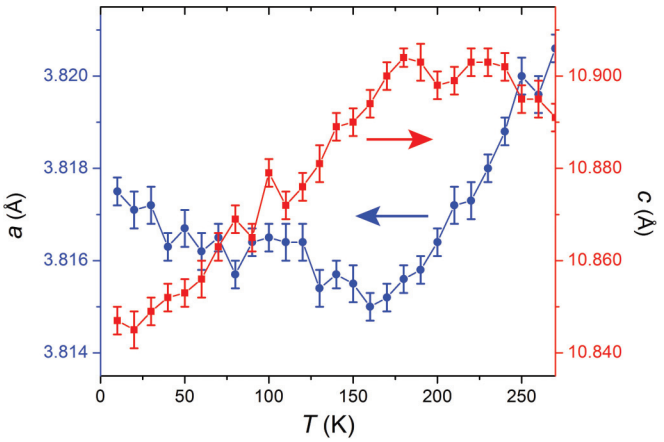

FIG. 2. (Color online) Temperature dependence of unit cell parameters a and c in the crystal structure of $La_{0.75}Pr_{0.25}Co_2P_2$.

IV. MAGNETIC PROPERTIES

A. Magnetometry

The magnetic measurements were carried out on an oriented single crystal of $La_{0.75}Pr_{0.25}Co_2P_2$, with the magnetic field directed parallel or perpendicular to the tetragonal c axis. Under a small applied field (0.01 T), the material demonstrates strong anisotropy of magnetic properties [Fig. 3(a)]. A magnetic phase transition that takes place at $T_{C1} = 167$ K results in easy magnetization in the ab plane and hard magnetization along the c axis. (In the following, we will refer to these magnetization directions as perpendicular $M_\perp$ and parallel $M_\parallel$, respectively.) This behavior suggests that the Co magnetic moments are ordered ferromagnetically and parallel to the ab plane, similar to the magnetically ordered structure reported for pure $LaCo_2P_2$.[10] At the point of the second magnetic transition, $T_{C2} = 66$ K, M shows a slight increase while M exhibits an abrupt drop and approaches zero at ~60 K. Below this temperature, M remains close to zero, but M shows a drop below $T_{C3} = 35$ K, indicating the third magnetic transition. By comparing the magnetic behavior of $La_{0.75}Pr_{0.25}Co_2P_2$ to that of $LaCo_2P_2$ and $PrCo_2P_2$, one might expect the transitions at 66 and 35 K to involve both Co and Pr magnetic moments.

The three magnetic phase transitions are supported by heat capacity measurements. The magnetic component of the heat capacity $C_p{}^m$ was obtained by subtracting the nonmagnetic contribution estimated by measuring the heat capacity of the paramagnetic isostructural compound $LaFe_{0.5}Co_{1.5}P_2$.[15] Anomalies at ~167, 66, and 35 K are evident in the temperature dependence of $C_p{}^m$, as well as in the temperature dependence of resistivity [Fig. 3(b)]. The coincidence of these anomalies with the ones observed in magnetic measurements justifies the assignments of the corresponding temperatures as critical points of magnetic phase transitions. The T_{C1} and T_{C2} values were determined as the inflection points of the $M_\parallel$ vs T curve while the T_{C3} value was taken as equal to the low-temperature maximum of the $M_\perp$ vs T curve [Fig. 3(a)].

An examination of isothermal field-dependent magnetization measured at 120 and 35 K, shown in Fig. 4 by blue and red curves, respectively, clearly demonstrates the change in the character of magnetic anisotropy. The c direction is a hard axis at higher temperatures but becomes an easy axis at lower

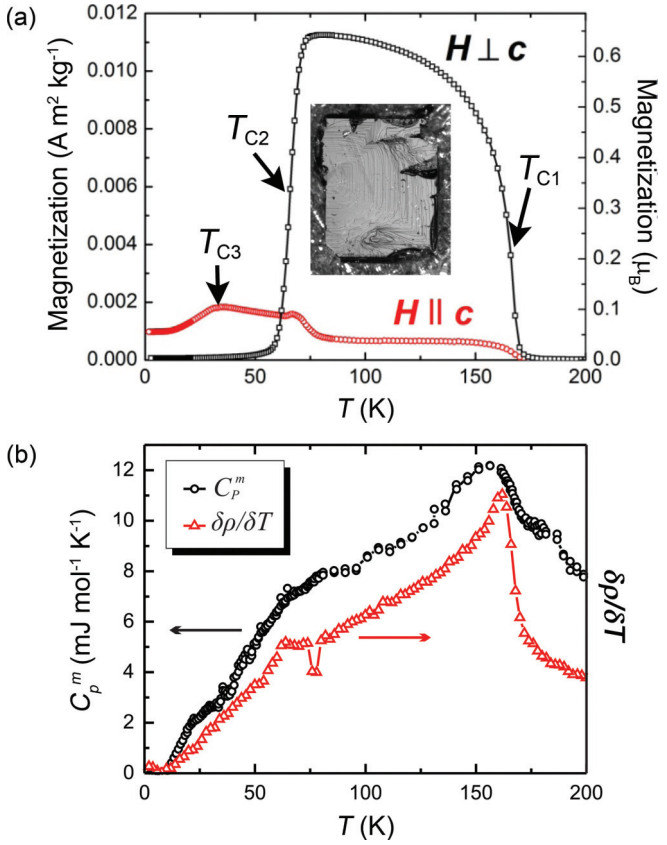

FIG. 3. (Color online) (a) Temperature dependence of magnetization measured on a single crystal of $La_{0.75}Pr_{0.25}Co_2P_2$ in the field-cooled mode, with the magnetic field of 0.01 T applied parallel (red curve) and perpendicular (black curve) to the c axis. The inset shows the surface of the single crystal viewed along the c axis. This crystal was used for MOI. (b) Temperature dependences of the magnetic component of the heat capacity and the first derivative of electrical resistivity for $La_{0.75}Pr_{0.25}Co_2P_2$.

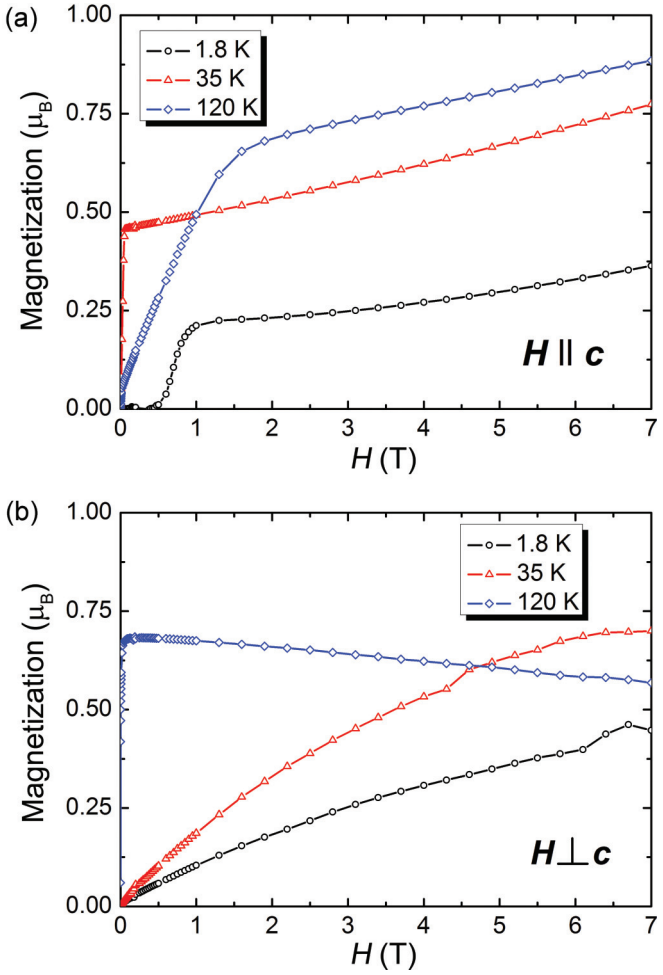

FIG. 4. (Color online) Isothermal field dependences of magnetization for a single crystal of $La_{0.75}Pr_{0.25}Co_2P_2$ measured with the magnetic field parallel (a) and perpendicular (b) to the c axis.

temperatures. The change in the easy magnetization direction is also evident from the field-dependent data (hysteresis) collected at 100 and 5 K, although significant remanence is observed only at the lower temperature (Fig. 5). The difference in remanence is related to the large magnetocrystalline anisotropy of the Pr sublattice that is not ordered at 100 K.

The maximum value of parallel magnetization observed at 35 K is lower than that at 120 K, and the maximum parallel magnetization at 1.8 K is even lower. These observations suggest that the Pr magnetic moments order antiparallel to the Co magnetic moments, leading to the decrease in the total magnetization below T_{C2}. The lower parallel magnetization at 1.8 K as compared to that at 35 K suggests additional reorientation of the magnetic moments, perhaps a transition from a noncollinear to a collinear ferrimagnetic structure. We will return to this question in Sec. V once the results obtained by other characterization methods have been described.

B. Magneto-optical imaging

To further investigate the modification of magnetic anisotropy, we carried out MOI on the surface of the single crystal of $La_{0.75}Pr_{0.25}Co_2P_2$. MOI allows direct observation of the formation of magnetic domains and reveals local features of magnetization process, which are unattainable from bulk magnetization measurements. This imaging technique employs Bi-doped garnet indicator films with in-plane magnetization, which are sensitive to the distribution of magnetic fields at the surface of a magnetic material.[21–23] The magnitude of the magnetic moment along the viewing direction is responsible for the intensity of the magneto-optical signal, while the change in the orientation of the total moment between different domains provides the imaging contrast.

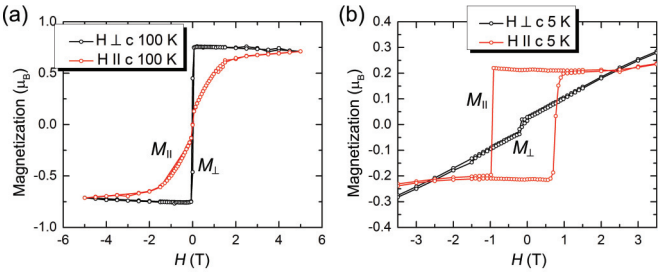

FIG. 5. (Color online) Magnetic hysteresis loops measured on a single crystal of $La_{0.75}Pr_{0.25}Co_2P_2$ at 100 K (a) and 5 K (b) with the magnetic field applied parallel (red curves) and perpendicular (black curves) to the c axis.

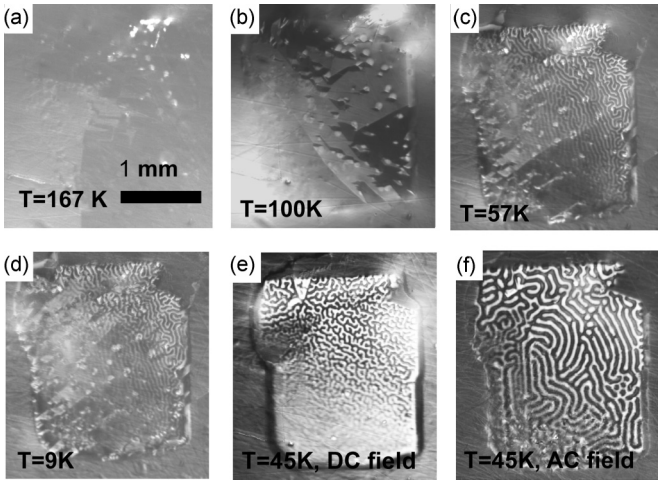

FIG. 6. Magneto-optical images taken on a single crystal of $La_{0.75}Pr_{0.25}Co_2P_2$ oriented with the c axis along the optical axis of the microscope. Temperature-dependent patterns were recorded upon cooling from room temperature in a zero magnetic field (a–d) or in a parallel applied field of 0.18 T (e). (f) Pattern obtained after applying a parallel ac magnetic field of 0.010 T at a frequency of 100 Hz and a temperature of 45 K.

The single crystal of $La_{0.75}Pr_{0.25}Co_2P_2$ was oriented with the c axis along the optical axis of the microscope [Fig. 3(a), inset] and cooled in a zero applied magnetic field from 300 K to $T_{C1} = 167$ K. The nucleation of individual magnetic domains was observed at 167 K [Fig. 6(a)] and below due to spontaneous magnetization. The density of these new phase domains increases as the temperature goes down. As clearly seen in Fig. 6(b), recorded at 100 K, the domains have an irregular (triangular or rhombic) shape. Such a domain nucleation pattern indicates that magnetic moments of Co are not aligned exactly parallel to the ab plane but are slightly canted toward the c axis.

Below $T_{C2} = 66$ K, the magnetic structure is transformed to labyrinth domains [Fig. 6(c)]. The nucleation of these black and white domains, which have magnetization in opposite directions along the c axis, coincides with the sharp reduction of the perpendicular magnetization [Fig. 3(a)], thus confirming the switching of magnetic anisotropy at T_{C2}. As the temperature is decreased further, the labyrinth domain pattern becomes more pronounced. Its intensity, however, slightly weakens below 35 K [Fig. 6(d)], indicating the lower magnetic moment along the c axis, which is again in agreement with the magnetization data.

An examination of Fig. 6(c) and 6(d) also reveals that the formation of labyrinth domains is not uniform over the single crystal, which might be explained by the presence of impurities or defects that can pin magnetic moments, thus preventing the alignment of domains along the c axis. To nucleate domains more uniformly throughout the crystal, the sample was cooled down with an external field of 0.18 T applied along the c axis. The formation of domains became more pronounced yet remained incomplete even under these conditions [Fig. 6(e)]. Finally, an equilibrium domain pattern

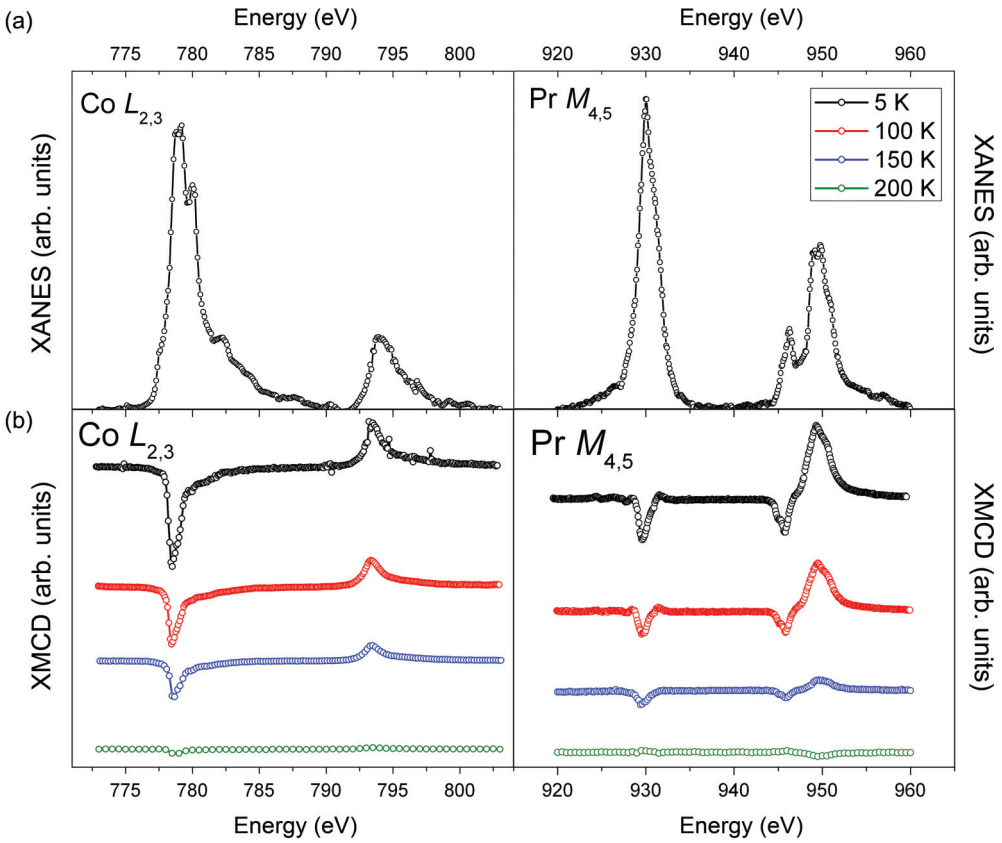

FIG. 7. (Color online) The 5-K XANES spectra (a) and variable-temperature XMCD spectra (b) measured at Co-$L_{2,3}$ and Pr-$M_{4,5}$ edges on a single crystal of $La_{0.75}Pr_{0.25}Co_2P_2$ with a 1-T magnetic field applied along the c axis.

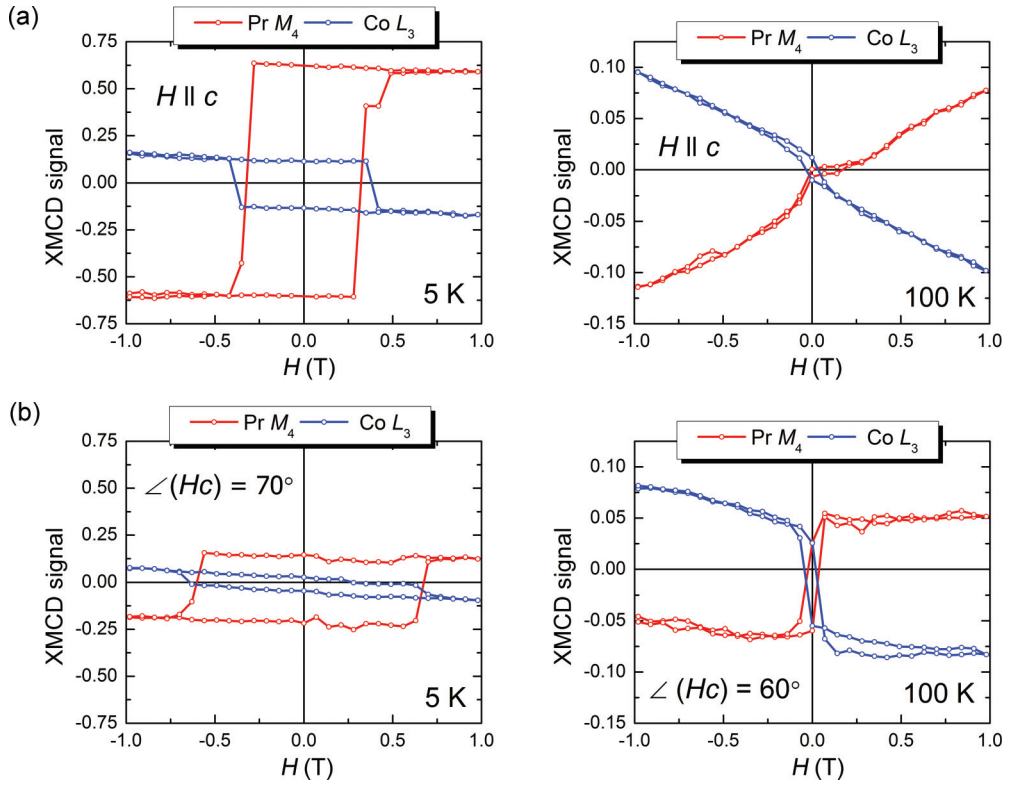

FIG. 8. (Color online) Field dependences of the integrated intensities of Co-L_3 and Pr-M_4 XMCD spectra measured on a single crystal of $La_{0.75}Pr_{0.25}Co_2P_2$ at 5 K (left) and 100 K (right), with the magnetic field direction parallel to the c axis (a) and inclined 70° or 60° to the c axis (b).

was achieved by applying an ac magnetic field of 0.01 T at the frequency of 100 Hz along the c direction [Fig. 6(f)].

V. MAGNETIC STRUCTURE

A. X-ray absorption spectroscopy

To probe directly the interaction between the Co and the Pr magnetic sublattices, we performed x-ray absorption spectroscopy studies on a single crystal of $La_{0.75}Pr_{0.25}Co_2P_2$. Variable-temperature XANES and XMCD spectra were collected under an applied magnetic field of 1 T. An examination of XANES spectra [Fig. 7(a)] indicates that Pr exists in the oxidation state of 3+, which can be readily distinguished by a characteristic fine structure of the spectrum.[24] The XMCD spectra reveal no signature of magnetic ordering in either the Co or the Pr sublattice at 200 K. (As will be shown below, a collinear antiferromagnetic ordering that is not detectable by XMCD was ruled out based on neutron diffraction studies.) At 150 K, however, a clear XMCD signal was observed at the Co $L_{2,3}$ edge, indicating the ordering of Co magnetic moments. The relatively weak signals observed in the Pr $M_{4,5}$ channel at 150 and 200 K and in the Co $L_{2,3}$ channel at 200 K are attributed to the field-induced paramagnetic response. Strong Co and Pr XMCD signals were observed at 100 and 5 K, indicating that both magnetic sublattices are ordered at these temperatures in the applied field of 1 T.

To determine the orientation of Co and Pr magnetic moments with respect to the tetragonal c axis in the low-temperature range, hysteresis XMCD curves were recorded for both elements with the field oriented either parallel or at 70° (at 5 K) and 60° (at 100 K) with respect to the c axis. (The experimental setup did not allow the measurement of the XMCD spectrum with the field perpendicular to the c axis.) An examination of the XMCD spectra recorded at 5 K clearly reveals the preferential alignment of Co and Pr moments along the c axis, as the absolute values of the XMCD signals are maximized for $H \parallel c$ (Fig. 8). This direction, however, becomes a hard magnetization axis at 100 K. We also note the substantially larger hysteresis at 5 K, which underscores that the ordering in the Pr sublattice imparts higher anisotropy to the magnetic properties in this system. These observations are in good agreement with the results of magnetic and magneto-optical measurements.

B. Neutron diffraction

The lattice parameters of $La_{0.75}Pr_{0.25}Co_2P_2$ refined from NPD data were in good agreement with those obtained from single-crystal x-ray diffraction (Table I). While x-ray diffraction cannot discriminate between La and Pr atoms, neutron diffraction is well suited for distinguishing these elements due to the large difference in the neutron scattering lengths of La (8.2 fm) and Pr (4.6 fm). The crystal structure refinement performed on the 220-K NPD data resulted in the composition $La_{0.79(4)}Pr_{0.21(4)}Co_2P_2$. The structural model obtained is in agreement with the statistical distribution of Pr and La atoms over the 2a Wyckoff positions, as we did not observe any superstructure reflections caused by ordering

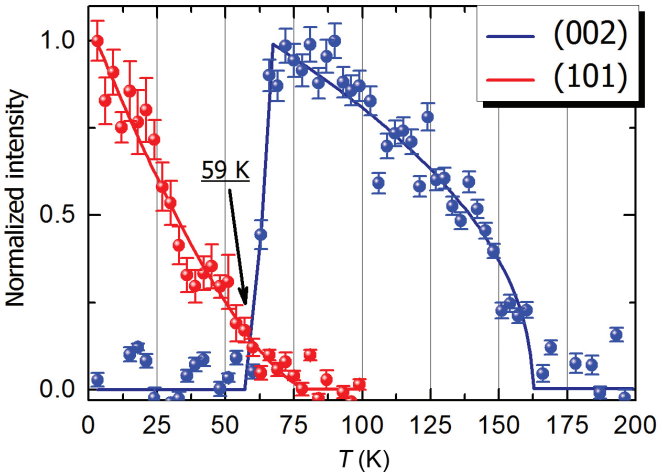

FIG. 9. (Color online) Temperature dependence of normalized intensity of NPD magnetic peaks (002) and (101) of $La_{0.75}Pr_{0.25}Co_2P_2$. Solid lines are visual guides.

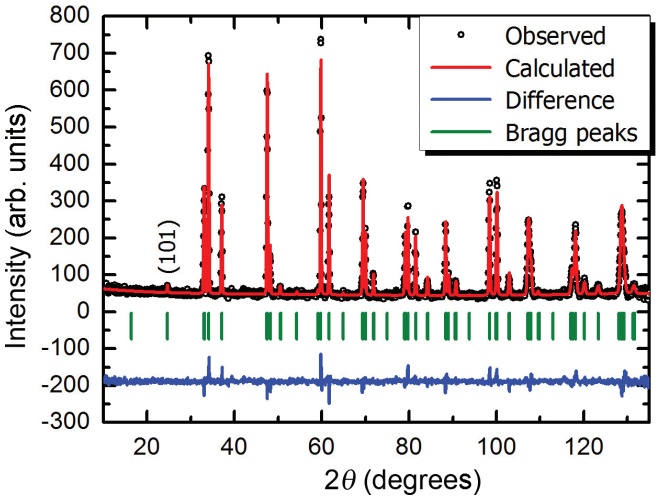

FIG. 10. (Color online) Rietveld refinement of the NPD pattern of $La_{0.75}Pr_{0.25}Co_2P_2$ collected at 4 K ($R_F = 0.0675$, $\chi^2 = 1.85$).

of the rare-earth atoms. For further analysis of the low-temperature data, the composition was fixed to the nominal value of $La_{0.75}Pr_{0.25}Co_2P_2$ to avoid additional correlations between the refined parameters.

The NPD pattern recorded at 4 K in the absence of an applied magnetic field revealed a strong (101) reflection, while the pattern collected at 100 K showed a small hump at the position calculated for the (002) reflection. Both (002) and (101) peaks were absent in the NPD pattern collected at 220 K. The temperature dependence of the intensity of these reflections was monitored using the HB-1A triple-axis spectrometer (Fig. 9).

Neither (002) nor (101) reflection violates the centering condition for the $I4/mmm$ space group. Therefore, one can exclude symmetry-breaking antiferromagnetic ordering within either the Co or the Pr sublattice. An analysis of possible magnetic structure models compatible with the $k = (0,0,0)$ propagation vector revealed that the (002) and (101) magnetic peaks correspond to the collinear ordering of magnetic moments perpendicular and parallel to the c axis, respectively.

The results of magnetic measurements and XMCD spectroscopy, along with the knowledge of magnetic behavior of $LaCo_2P_2$ and $PrCo_2P_2$, strongly suggest that the magnetic phase transition in $La_{0.75}Pr_{0.25}Co_2P_2$ at $T_{C1} = 167$ K is due to the ordering of Co moments only, while the lower-temperature phase transitions are associated with both Co and Pr sublattices. Consequently, we attribute the (002) peak observed in the zero-field NPD patterns collected below T_{C1} to the ordering of Co magnetic moments parallel to the ab plane. The drop in the intensity of the (002) peak that vanishes at ~60 K can be associated with the realignment of Co magnetic moments along the c axis. One should note that the (hkl) reflection condition, $l = 2n$, associated with the Co site (Wyckoff position $4d$:0, 1/2, 1/4), disallows the contribution of Co moment to the (101) reflection; therefore, the intensity of this peak represents a direct measure of the order parameter for the Pr sublattice. It is obvious from Fig. 9 that the initial growth of the (101) peak intensity coincides with the decrease in (002) peak intensity. Therefore, the reorientation of the Co moments occurs simultaneously with the ordering of the Pr moments at $T_{C2} = 66$ K.

Fitting the NPD data collected at 96 K to the model of Co moments ordered ferromagnetically in the ab plane resulted in the magnetic moment of $0.38(7)\mu_B$ per Co atom, which is in good agreement with the value of $0.36\mu_B$ calculated from the magnetic hysteresis curve at 100 K [Fig. 5(a)]. The refinement of the NPD pattern collected at 4 K was performed with an assumption of antiparallel alignment of Pr and Co magnetic moments along the c axis, as suggested by the results of magnetic measurements. Due to the limited number of magnetic peaks observed at this temperature, the Co magnetic moment was fixed to the value of $0.38\mu_B$. The refinement resulted in a satisfactory fit of diffraction data (Fig. 10) with a Pr magnetic moment of $3.12(4)\mu_B$, which is close to the theoretically expected value of $3.20\mu_B$. It is worth noting that the refined value of the Pr moment is also fully consistent with the results of single-crystal magnetization measurements performed at 1.8 K, as shown in Fig. 4(a) (i.e., the isothermal field dependence measured with the magnetic field oriented parallel to the c axis). As such, the 25% of $3.12\mu_B$ corresponding to the Pr contribution to net magnetization is almost compensated by the $2 \times 0.38\mu_B$ magnetization due to Co spins in the suggested collinear ferrimagnetic structure.

C. Neutron diffraction in an applied magnetic field

According to the magnetic measurements, a change of the easy magnetization direction should occur at the crossover point between the parallel and the perpendicular magnetization, i.e., at 59 K [Fig. 3(a)]. To directly confirm this expectation, we performed variable-temperature NPD experiments on loose powder of $La_{0.75}Pr_{0.25}Co_2P_2$ in the magnetic field of 0.25 T applied perpendicular to the horizontal neutron scattering plane. At intermediate temperatures, between T_{C1} and T_{C2}, the alignment of Co moments in the ab plane should cause preferential orientation of crystallites with the ab plane along the magnetic field and perpendicular to the neutron beam, i.e., the c axis will be oriented in the scattering plane (Fig. 11). At temperatures below T_{C2}, the alignment

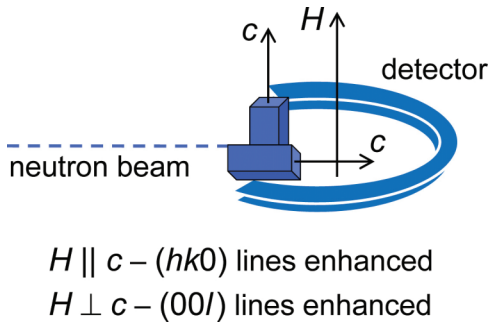

FIG. 11. (Color online) The typical experimental setup in the scattering experiments on the HB-2A neutron powder diffractometer.

of Co and Pr moments along the c axis should lead to reorientation of crystallites, with the c axis parallel to the field and perpendicular to the scattering plane. Indeed, a pronounced texturing effect is observed in the neutron diffraction patterns (Fig. 12): (hkl) reflections with smaller h and k and larger l indices gain higher intensity in the range between T_{C1} and T_{C2}, while ($hk0$) reflections are enhanced below T_{C2}, in agreement with the expected orientation of the c axis out of the neutron scattering plane at lower temperatures.

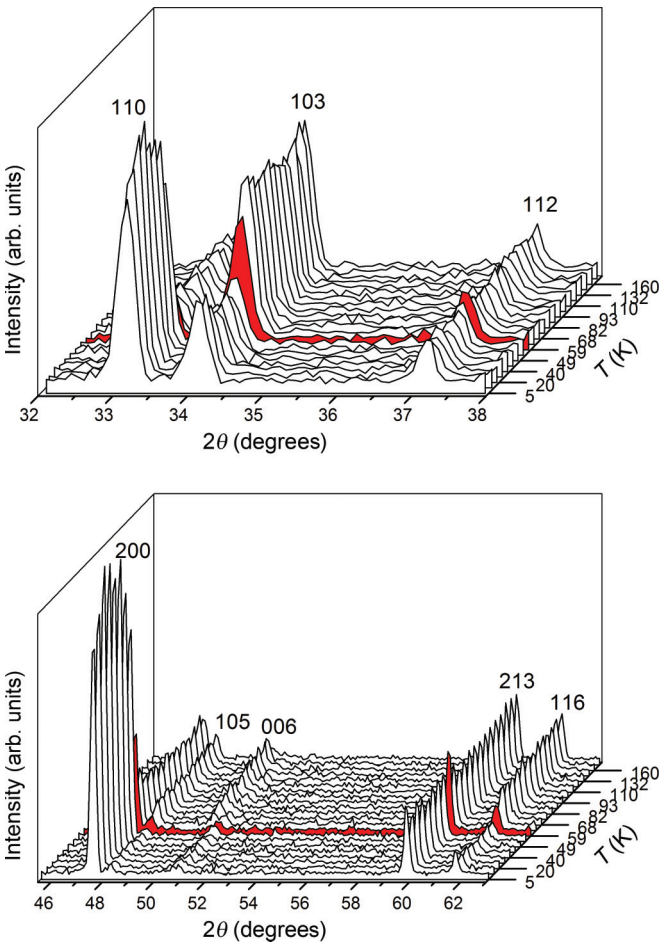

FIG. 12. (Color online) Fragments of variable-temperature NPD patterns collected on loosely packed powder of $La_{0.75}Pr_{0.25}Co_2P_2$ in an applied magnetic field of 0.25 T. Note the crossover point at 59 K (highlighted in red).

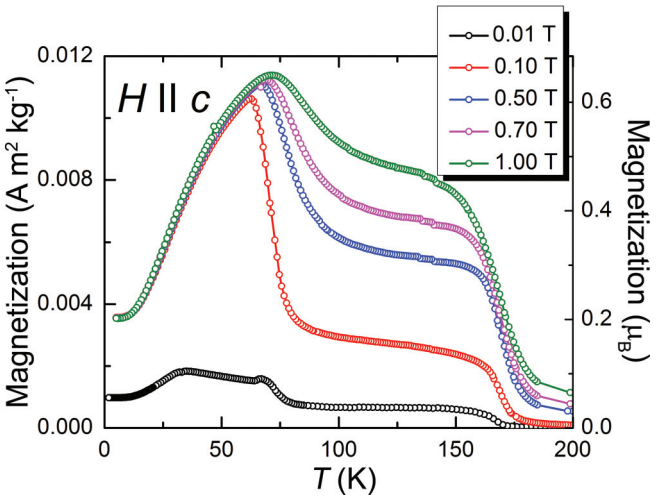

FIG. 13. (Color online) Isofield temperature dependence of magnetization measured on a single crystal of $La_{0.75}Pr_{0.25}Co_2P_2$ at various magnetic fields applied parallel to the c axis in the field-cooled regime.

D. Field-dependent magnetic behavior

One might note a seeming discrepancy among the results of magnetic measurements, neutron diffraction, and XMCD spectroscopy. The first two methods indicate the ordering of Pr magnetic moments and reorientation of Co magnetic moments at $T_{C2} = 66$ K (Figs. 3 and 9), while the XMCD technique suggests that the Pr sublattice is already significantly ordered at 100 K (Fig. 7). It should be kept in mind, however, that the NPD was performed in a zero-applied magnetic field, while the temperature-dependent magnetic data were obtained in a rather weak applied field of 0.010 T. In contrast, the XMCD spectra were acquired under a much higher field (1 T), which likely increases the ordering temperature. To confirm this assumption, we measured the temperature dependence of field-cooled magnetization at different fields applied parallel to the c axis, in analogy to the XMCD spectra shown in Fig. 7. The magnetization below T_{C1} gradually increases for higher magnetic fields, as would be expected for stronger canting of ferromagnetically ordered Co moments out of the ab plane, while the lower-temperature maximum of magnetization (T_{C2}) caused by ferrimagnetic ordering of Co and Pr moments along the c axis is gradually shifted to higher temperatures as the field is increased (Fig. 13).

VI. CONCLUDING REMARKS

The rich magnetic behavior demonstrated by $La_{0.75}Pr_{0.25}Co_2P_2$ is in significant contrast to the rather simple magnetism of its ternary congeners, $LaCo_2P_2$ and $PrCo_2P_2$. The magnetic phase transitions in the Co and Pr sublattices of $PrCo_2P_2$ are uncoupled from each other, occurring at 305 and 19 K, respectively, and resulting in antiferromagnetic ordering for each element, with the moments aligned along the c axis of the tetragonal structure. $LaCo_2P_2$, on the other hand, exhibits ferromagnetic ordering of Co moments in the ab plane at 132 K. In $La_{0.75}Pr_{0.25}Co_2P_2$, however, neither sublattice exhibits an antiferromagnetic order, and a magnetic phase transition in one sublattice has a dramatic influence on the behavior of the other sublattice, resulting in the

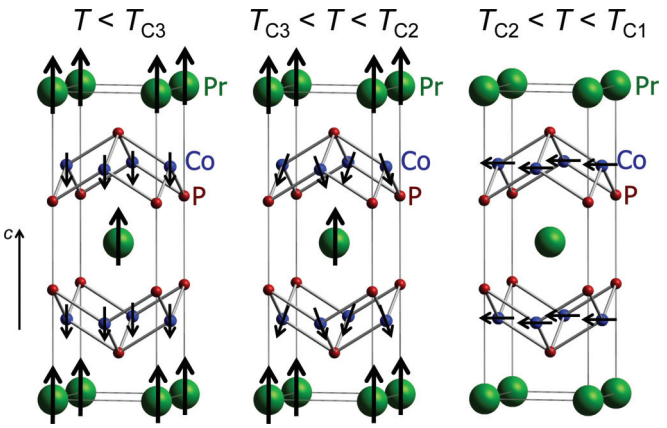

FIG. 14. (Color online) Proposed magnetic structures of $La_{0.75}Pr_{0.25}Co_2P_2$ in different temperature ranges between the critical points of magnetic phase transitions.

temperature-dependent modification of the total magnetic anisotropy (Fig. 14). The magnetic behavior of $La_{0.75}Pr_{0.25}Co_2P_2$ thus bridges the gap between $LaCo_2P_2$ and $PrCo_2P_2$ in a unique and fascinating way.

A combined study of $La_{0.75}Pr_{0.25}Co_2P_2$ by means of magnetic measurements, MOI, x-ray absorption spectroscopy, and neutron diffraction has unequivocally shown that (1) the Co magnetic moments undergo ferromagnetic ordering in the *ab* plane at $T_{C1} = 167$ K, in a manner akin to the ferromagnetic phase transition in $LaCo_2P_2$; (2) the Pr magnetic moments undergo ferromagnetic ordering at $T_{C2} = 66$ K; (3) the ordering of Pr moments at $T_{C2} = 66$ K is accompanied by simultaneous reorientation of Co moments in the direction opposite to that of the Pr moments; (4) similar to $PrCo_2P_2$, both Pr and Co magnetic moments are aligned along the *c* axis below T_{C2} but the ordering within each sublattice is ferromagnetic rather than antiferromagnetic; (5) below T_{C2}, the Co moments are not oriented exactly antiparallel to the Pr moments; and (6) below $T_{C3} = 35$ K, the moments reorient further to provide for more pronounced antiferromagnetic $3d$-$4f$ coupling, as suggested by the decrease in the total magnetization, the weakening of the magneto-optical contrast of the labyrinth domain structure, and the smaller saturation magnetization at 1.8 K relative to 35 K.

In the context of these findings, we especially would like to point out two features observed in the magnetism of $La_{0.75}Pr_{0.25}Co_2P_2$. First, despite the relatively low content of Pr, the ordering in the Pr sublattice takes place at 70 K, which is much higher than the Pr-ordering temperature reported for $PrCo_2P_2$ (19 K). This is not surprising, however, if one takes into account the ferromagnetic ordering in the Co sublattice at 167 K in $La_{0.75}Pr_{0.25}Co_2P_2$. Hence, in this compound, the Co sublattice causes an effective internal field that forces the ordering of Pr moments at much higher temperatures than in $PrCo_2P_2$, where the total moment of the Co sublattice becomes vanishingly small due to antiferromagnetic ordering of Co moments at 305 K. Second, in $La_{0.75}Pr_{0.25}Co_2P_2$, the reorientation of the Co moments along the *c* axis at 66 K is obviously coupled to the ordering of Pr moments at the same temperature. Thus, the remarkable magnetic properties of $La_{0.75}Pr_{0.25}Co_2P_2$ emerge from the strong mutual influence of both magnetic sublattices due to $3d$-$4f$ coupling, a behavior that is not observed for any ternary RCo_2P_2 material.

The character of the $3d$-$4f$ coupling also deserves to be mentioned. Extensive studies of RCo_2, a related group of intermetallics built of alternating layers of rare-earth and cobalt atoms, conclusively established that the $3d$ moments of Co couple ferromagnetically to $4f$ moments of lighter rare-earth metals and antiferromagnetically to $4f$ moments of heavier rare-earth metals.[25] The interaction between the $3d$ and the $4f$ moments in $La_{0.75}Pr_{0.25}Co_2P_2$ shows an opposite trend. This observation might indicate an important role played by the nonmetal P atoms in defining the character of the $3d$-$4f$ magnetic exchange in this and related compounds of the RCo_2P_2 series. We are currently investigating this aspect of their magnetism using both theoretical and experimental methods. Results of these studies will be reported in due course.

ACKNOWLEDGMENTS

M.S. thanks the National Science Foundation (Career Award No. DMR-0955353) for the support of this work. Experiments at the Oak Ridge National Laboratory's High Flux Isotope Reactor were sponsored by the Scientific User Facilities Division, Office of Basic Energy Sciences, U.S. Department of Energy (DOE). Use of the Advanced Photon Source, an Office of Science User Facility operated for the U.S. DOE Office of Science by Argonne National Laboratory, was supported by the U.S. DOE under Contract No. DE-AC02-06CH11357. We thank Dr. Richard Rosenberg and Dr. Yongseong Choi (Argonne National Laboratory, Advanced Photon Source) for assistance with XMCD experiments, as well as Dr. Javier Fernandez-Rodriguez for the calculation of the theoretical XANES spectrum for the Pr^{3+} ion.

*Present address: Department of Chemistry, University of California, Davis, California 95616, USA.
†Present address: Department of Chemistry, McMaster University, 1280 Main Street West, Hamilton, Ontario, Canada L8S 4M1.
‡Present address: Department of Physics, University of Tennessee at Knoxville, Knoxville, Tennessee 37996, USA.
§Corresponding author: shatruk@chem.fsu.edu.

[1] M. Rotter, M. Tegel, and D. Johrendt, Phys. Rev. Lett. **101**, 107006 (2008).
[2] Z.-A. Ren, W. Lu, J. Yang, W. Yi, X.-L. Shen, C. Zheng, G.-C. Che, X.-L. Dong, L.-L. Sun, F. Zhou, and Z.-X. Zhao, Chin. Phys. Lett. **25**, 2215 (2008).
[3] P. C. Canfield and S. L. Bud'ko, Annu. Rev. Condens. Matter Phys. **1**, 27 (2010).
[4] K. Kovnir and M. Shatruk, Eur. J. Inorg. Chem. **2011**, 3955 (2011).
[5] C. Zheng and R. Hoffmann, J. Solid State Chem. **72**, 58 (1988).
[6] D. Johrendt, C. Felser, O. Jepsen, O. K. Andersen, A. Mewis, and J. Rouxel, J. Solid State Chem. **130**, 254 (1997).

[7]A. Szytula and J. Leciejewicz, in *Handbook on the Physics and Chemistry of Rare Earths*, edited by K. A. Gschneidner, Jr., and L. Eyring (Elsevier Science Publishers, Amsterdam, 1989), Vol. 12, p. 133.
[8]H. Fujii, T. Okamoto, T. Shigeoka, and N. Iwata, Solid State Comm. **53**, 715 (1985).
[9]M. Reehuis and W. Jeitschko, J. Phys. Chem. Solid. **51**, 961 (1990).
[10]M. Reehuis, C. Ritter, R. Ballou, and W. Jeitschko, J. Magn. Magn. Mater. **138**, 85 (1994).
[11]M. Reehuis, P. J. Brown, W. Jeitschko, M. H. Möller, and T. Vomhof, J. Phys. Chem. Solid. **54**, 469 (1993).
[12]M. Reehuis, W. Jeitschko, G. Kotzyba, B. Zimmer, and X. Hu, J. Alloys Compd. **266**, 54 (1998).
[13]K. Kovnir, C. M. Thompson, H. D. Zhou, C. R. Wiebe, and M. Shatruk, Chem. Mater. **22**, 1704 (2010).
[14]K. Kovnir, W. M. Reiff, A. P. Menushenkov, A. A. Yaroslavtsev, R. V. Chernikov, and M. Shatruk, Chem. Mater. **23**, 3021 (2011).
[15]K. Kovnir, V. O. Garlea, C. M. Thompson, H. D. Zhou, W. M. Reiff, A. Ozarowski, and M. Shatruk, Inorg. Chem. **50**, 10274 (2011).
[16]S. Jia, S. Chi, J. W. Lynn, and R. J. Cava, Phys. Rev. B **81**, 214446 (2010).
[17]S. Jia, P. Jiramongkolchai, M. R. Suchomel, B. H. Toby, J. G. Checkelsky, N. P. Ong, and R. J. Cava, Nat. Phys. **7**, 207 (2011).
[18]L. G. Akselrud, P. Y. Zavalii, Y. Grin, V. K. Pecharski, B. Baumgartner, and E. Wölfel, Mater. Sci. Forum **133–136**, 335 (1993).
[19]V. O. Garlea, B. C. Chakoumakos, S. A. Moore, G. B. Taylor, T. Chae, R. G. Maples, R. A. Riedel, G. W. Lynn, and D. L. Selby, Appl. Phys. A **99**, 531 (2010).
[20]J. W. Freeland, J. C. Lang, G. Srajer, R. Winarski, D. Shu, and D. M. Mills, Rev. Sci. Instr. **73**, 1408 (2002).
[21]A. A. Polyanskii, X. Y. Cai, D. M. Feldmann, and D. C. Larbalestier, in *Nano-Crystalline and Thin Film Magnetic Oxides*, NATO Science Partnership Subseries: 3, Vol. 72, edited by I. Nedkov and M. Ausloos (Kluwer Academic Publishers, Dordrecht, 1999), p. 353.
[22]A. A. Polyanskii, D. M. Feldmann, and D. C. Larbalestier, in *Handbook of Superconducting Materials*, edited by D. A. Cardwell and D. S. Ginley (IOP Publishing, Bristol, Philadelphia, 2003), p. 1551.
[23]A. Polyanskii, X. L. Wang, Q. W. Yao, S. X. Dou, Z. W. Lin, and J. G. Zhu, J. Appl. Phys. **99**, 08A704 (2006).
[24]M. Zhuravleva, S. Friedrich, and C. L. Melcher, Appl. Phys. Lett. **101**, 101902 (2012).
[25]N. H. Duc and P. E. Brommer, Handb. Magn. Mater. **12**, 259 (1999).